Materials Science and Engineering A 524 (2009) 151–157

Contents lists available at ScienceDirect

Materials Science and Engineering A

journal homepage: www.elsevier.com/locate/msea

Ageing and work-hardening behaviour of a commercial AA7108 aluminium alloy

Ida Westermann[a,*], Odd Sture Hopperstad[a], Knut Marthinsen[b], Bjørn Holmedal[a,b]

[a] *Structural Impact Laboratory (SIMLab) - Centre for Research-based Innovation and Department of Structural Engineering, Norwegian University of Science and Technology, NO-7491, Trondheim, Norway*
[b] *Department of Material Science and Engineering, Norwegian University of Science and Technology, NO-7491 Trondheim, Norway*

ARTICLE INFO

Article history:
Received 6 April 2009
Received in revised form 9 June 2009
Accepted 11 June 2009

Keywords:
Aluminium alloys
Work-hardening
Artificial ageing
Precipitate free zones

ABSTRACT

In the 7xxx aluminium alloying system several mechanisms influence the hardening behaviour of the alloys, e.g. particle size and distribution, dislocation density and alloying elements in solid solution. This work is an experimental study of ageing and work-hardening considering a commercial AA7108 alloy in the as-cast and homogenized condition. Tensile specimens have been exposed to a solution heat treatment and a two-step age-hardening treatment with varying time at the final temperature. The tensile data for the different tempers have been evaluated in elucidation of already existing models based on a one-parameter framework. The precipitate size and distribution have been further investigated in the transmission electron microscope for a selection of tempers, and the influence of these parameters on the work-hardening behaviour has been discussed.

1. Introduction

The combination of high specific strength and ductility makes aluminium an exceptional material for energy absorption, and the high strength aluminium alloys are therefore well suitable in car bumper systems designed to absorb energy in a collision. The 7xxx alloying systems belong to the heat-treatable alloys which owe their strength to the combination of work-hardening, precipitation-hardening, and alloying elements in solid solution. The mechanical properties of these alloys are strongly dependent on the thermo-mechanical process and it is therefore important to understand the relationship between the microstructure evolution during thermo-mechanical processing and the mechanical properties.

Several work-hardening models have been proposed for predicting the mechanical properties. A one-parameter model was introduced by Kocks in 1976 [1], a model that has been further refined by Mecking and Kocks [2] and Estrin and Mecking [3]. This model only takes the overall dislocation density of the material into account. Other work-hardening models, which include more detailed dislocation parameters, have later been introduced and used by other authors, see e.g. [4–7].

In materials containing precipitates, like the heat-treatable aluminium alloys, the interaction between precipitates and dislocations is of great importance. In general this interaction may be split into two cases, dependent on the size of the precipitates: (i) shearable precipitates, where the dislocations are able to cut through the precipitates, and (ii) non-shearable precipitates, where the precipitates become too large an obstacle and the dislocations will have to either climb or leave a dislocation loop around the precipitate. Due to the complexity of combining the two hardening phenomena, the one-parameter approach by Kocks, Mecking and Estrin has been used by several authors to model the influence of precipitates on the work-hardening behaviour, see e.g. [8–12]. An important result reported in the paper of Cheng et al. [12] is that the slope of the Kocks–Mecking curve, i.e. the derivative of the work-hardening rate with respect to stress, $d\theta/d\sigma$, which they assumed to remain approximately constant during plastic straining, can be used as a parameter to determine the transition from shearable to non-shearable precipitates. They concluded that this transition occurred at the peak strength for an AA7030 alloy, whereas it occurred in the overaged condition for an AA6111 alloy.

The present work is a study of a commercial AA7108 aluminium alloy heat treated to different tempers and the effect of particles on the work-hardening rate in the plastic regime. Both microstructure and mechanical properties are investigated and the data are evaluated in elucidation of the Cheng et al. approach [12]. This model has been chosen here, since it with a simple one-parameter representation of the dislocation density gives a good description of the work-hardening behaviour, still avoiding the mathematical complexity of multi-parameter model approaches. Note that another physical interpretation of the stress term contributions, as described, e.g. in [6], has shown to give a similarly good description by a three-parameter approach [7].

* Corresponding author. Fax: +47 73594701.
E-mail address: ida.westermann@ntnu.no (I. Westermann).

0921-5093/$ – see front matter © 2009 Elsevier B.V. All rights reserved.
doi:10.1016/j.msea.2009.06.036

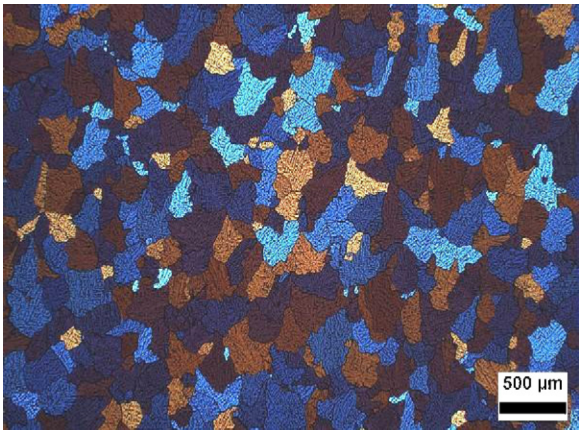

Fig. 1. Microstructure of the as-cast material.

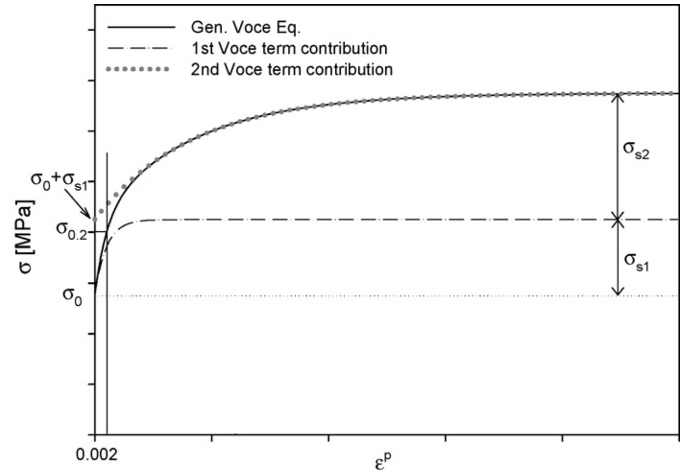

Fig. 2. The interpretation of the two terms in the generalized Voce equation.

2. Material and experimental procedure

A commercial AA7108 aluminium alloy was provided by Hydro Aluminium Structures Raufoss a.s. as an as-cast and homogenized extrusion ingot. Plastically deformed materials, such as extruded profiles, are usually affected by the texture due to the forming process. To avoid this effect, the experimental work is carried out on the as-cast and homogenized material. Round standard tensile specimens with a gauge length of 25 mm were made from the centre region with tensile axes in the longitudinal direction of the ingot. The microstructure of the as-cast material is shown in Fig. 1. The specimens were given a multistep heat treatment to different tempers before testing, see Table 1. A solid solution heat treatment was followed by storage at room temperature and two-step artificial ageing. Tensile testing was carried out at a constant nominal strain rate of $10^{-2}\,s^{-1}$ immediately after the heat treatments.

Specimens of the 5h and 11d materials were prepared for transmission electron microscopy (TEM) investigations by mechanical grinding and punching of 3 mm discs followed by electropolishing in a double-jet Tenupol by a 33% nitric acid solution in methanol operated at −20 °C and 15 V. The samples were investigated in a JEOL JEM-2010 TEM operated at a nominal voltage of 200 kV.

3. Data processing

The true stress, σ, and true strain, ε, were calculated from the tensile tests, up to the ultimate tensile strength. The plastic strain may then be found as $\varepsilon^p = \varepsilon - \sigma/E$, where E is the Young's modulus. A generalized Voce equation was then fitted to the experimental hardening curve, using a least-squares algorithm, in the range between $\varepsilon^p = 0.002$ and the strain at ultimate stress:

$$\sigma = \sigma_0 + \sum_{i=1}^{2} \sigma_{si} \left(1 - \exp\left(-\frac{\theta_i}{\sigma_{si}}\varepsilon^p\right)\right), \qquad (1)$$

where σ_0 is a yield stress, and σ_{si} and θ_i are a saturation stress and a work-hardening rate, respectively. The fitted σ_0 is a back-extrapolated stress at zero plastic strain. The interpretation of the two terms of the generalized Voce equation is shown in Fig. 2. Based on Eq. (1) the work-hardening rate, θ, can be calculated as

$$\theta = \frac{d\sigma}{d\varepsilon^p} = \sum_{i=1}^{2} \theta_i \exp\left(-\frac{\theta_i}{\sigma_{si}}\varepsilon^p\right). \qquad (2)$$

It is underlined that we use the generalized Voce model here as a convenient representation of the experimental data.

Table 1
The multistep heat treatment to which the material has been subjected. The 9h temper corresponds to the peak aged condition and is listed in bold fonts.

Sample designation	Solution heat treatment 480 °C	Room temperature	100 °C	150 °C
W	20 min	–	–	–
1h100C	20 min	24 h	1 h	–
3h	20 min	24 h	5 h	3 h
5h	20 min	24 h	5 h	5 h
9h (peak)	**20 min**	**24 h**	**5 h**	**9 h**
19h	20 min	24 h	5 h	19 h
50h	20 min	24 h	5 h	50 h
11d	20 min	24 h	5 h	264 h

4. Results

The true stress–strain curves for the different tempers are shown in Fig. 3. With increasing ageing time the strength increases from the fully soft W temper before it starts to drop when the overaged state is reached. The W, 1h100C, and 11d tempers show a different work-hardening behaviour than the other tempers. This is more

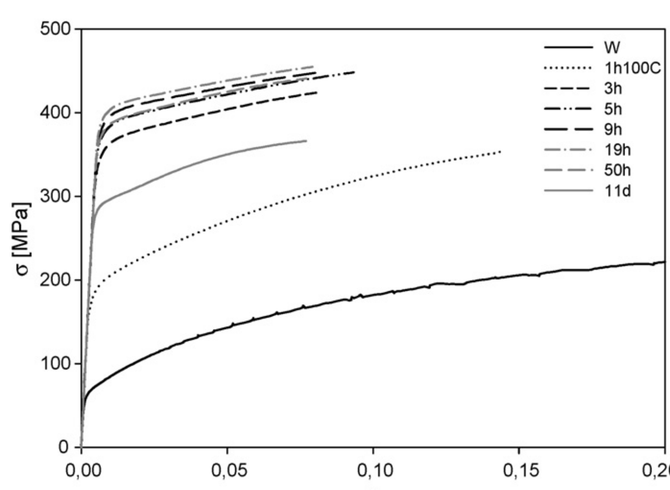

Fig. 3. True stress–strain curves for the different tempers to ultimate tensile strength.